FNAL TD Note # TD-08-011

April 02, 2008

Waveguide-Based Phase Shifter Performance Study

I. Gonin, T. Khabiboulinne, N. Soliak, and I. Terechkine

Motivations and design concept of a waveguide-based phase shifter for RF distribution system of the Proton Driver and first results of high power (up to 2 MW at 1300 MHz) test that proved the concept were described in [1] and [2]. Further increase of the RF power, as well as achievable phase shift, was limited by resonances at both ends of the frequency range. Sparking in the ferrite-loaded waveguide occurred when the working point (bias magnetic field) came close to one of the resonances. Although the achieved phase range was close to what was required for use of the shifter in the RF distribution network of the Proton Driver, understanding the nature of the resonant effects was considered very important because this knowledge would allow designing more efficient device. Besides the global hyro-magnetic resonance, the observed resonances in the vicinity of the working zone were often connected to some defects in positioning of the ferrite blocks, which ideally must be placed symmetrically relative to the waveguide's vertical and horizontal median planes. The resonances also could result from some difference in magnetic field in the two ferrite blocks of the shifter, or, maybe, were due to slight difference in the magnetic properties of the ferrite blocks.

The goal of this study was to identify all the resonances in the waveguide that restricted the working zone, to compare results of modeling with direct low level RF measurements, and to suggest ways of expanding the range of the device. The first part of the study was completed in September 2005; but the results were not published because the interest in this work (that was of crucial importance for the Proton Driver program back in 2005) has dropped dramatically following changes in the laboratory's strategic development plan. Corresponding cut of funding and new assignments prevented us from completing the study. Meanwhile similar studies continued in different laboratories around the globe resulting in development and successful testing of several vector modulators based on ferrite phase shifters [3, 4, and 5].

Some interest to the problem at FNAL was reborn as the X-project inherited the problems specific to the Proton Driver. Therefore, we decided to publish the results obtained back in 2005; this gives us a starting point to proceed with the second part of the agenda – implementing modifications that would render this approach useful for the program. Some work in this direction has already started and some results already exist; they will be published after a design concept of the device is fully developed.

I. Trapped modes in a waveguide loaded with ferrite blocks

A scheme representing cross-section view of the ferrite phase shifter prototype in [1] is shown in Fig. 1 below.

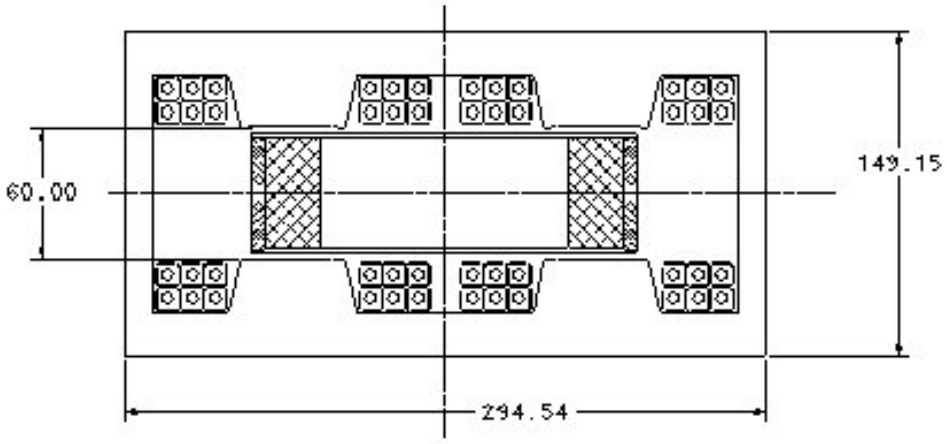

Figure 1: Phase shifter cross-section during power test.

The waveguide cross-section is 6.5" x 2" (165.1 x 50.8 mm^2). Working frequency of the device is 1300 MHz. For this waveguide size, the modes TE_{11}, TM_{11}, TE_{20}, TE_{21} etc. have higher critical frequencies. So, only TE_{10} mode can propagate along the waveguide; the critical wavelength of this mode is 330.2 mm (free space wavelength at 1300 MHz is 230.8 mm). The section of the waveguide loaded with the ferrite blocks (Yittrium Iron Garnet, YIG, type G510) attached to the side walls is 169 mm long. In this section, critical frequencies for all modes are shifted to lower values. So, some high order modes can be excited in this part of the waveguide if they are coupled with the main TE_{10} mode. If a mode existing in the ferrite-loaded section cannot propagate through a non-loaded part of the waveguide, it becomes trapped. As a result, if the quality factor of this virtual cavity is high, high electric field can be observed in the ferrite-loaded area.

Because the device is to work in the reflective mode (in combination with a "magic T" bridge), optimal position of the waveguide plug relative to the ferrite blocks must be found. This position differs depending on the blocks' shape and is of the order of 25 mm. Several configurations of the block cross-sections were studied. During the first high-power test [1], 20 mm thick rectangular cross-section blocks were used. Later the blocks were modified making them trapezoidal to reduce sparking and by reducing the thickness of the slabs to change resonant properties of the loaded waveguide (see Fig. 8 below).

Bias magnetic field in the blocks is created by using a frame magnetic circuit. Excitation coils are connected in series in a way that provides opposite directions of the magnetic field in the two blocks of the loaded section. Bias magnetic field in each gap of the magnetic system is related to the current in the main winding as

$$H\ (Oe) \approx 2.2 \cdot I\ (A)$$

With this field in the magnet gap, if the current I > 200 A, the magnetic flux density in the blocks

$$B\ (Gs) \approx 570 + 2.2 \cdot I\ (A)$$

For fine independent adjustment of the magnetic field in each ferrite block, correction coils were wound later on the peripheral part of the yoke (see Fig. 8). Each of two winding had 40 turns; the windings were connected in series so that the direction of the correction magnetic field was the same for the two blocks. In combination with the opposite direction of the main field, a differential shift in the bias field for the two YIG blocks could be obtained. This shift was ±8 Gs for 1 A of the compensation coil current.

It worth to mention here that it appeared important to have direction of the magnetic filed in the two blocks anti-parallel. If the magnetic field vectors were parallel, additional resonances could take place because of the circular polarization of the magnetic field vector. RF properties of the ferrite material depend on the direction of RF wave propagation, which defines the direction of the magnetic field rotation in each ferrite block, and bias magnetic field vector, which defines the direction of the spin precession. Because the circular polarization is opposite for the two sides of the waveguide, the opposite direction of the magnetic field in the blocks results in both sides of the waveguide working in a similar way. In this case, both sides of the waveguide show identical propagation properties for the direct and reflected waves, thus eliminating resonance conditions for some of resonances. It is necessary to say though that for each block RF properties for the direct wave will be different from that for the reflected wave. If the bias field is unidirectional, the circular polarized component sees similar material properties when moving through one of the blocks in the forward direction and through another block in the opposite direction. Thus, a resonance condition can be met through a ‘cross- talk’ between the different sides of the ferrite-loaded waveguide. Fig. 2 below demonstrates excitation of one of this type of resonances at 1292 MHz. Far from this resonant frequency, at 1266 MHZ, the wave field distribution is identical for both blocks. At 1292 MHz with parallel bias field a resonant condition exists; it disappears if anti-parallel bias field is applied. Poynting vector diagram on

the right of Fig. 2 demonstrates the energy flow in the form of the "cross talk".

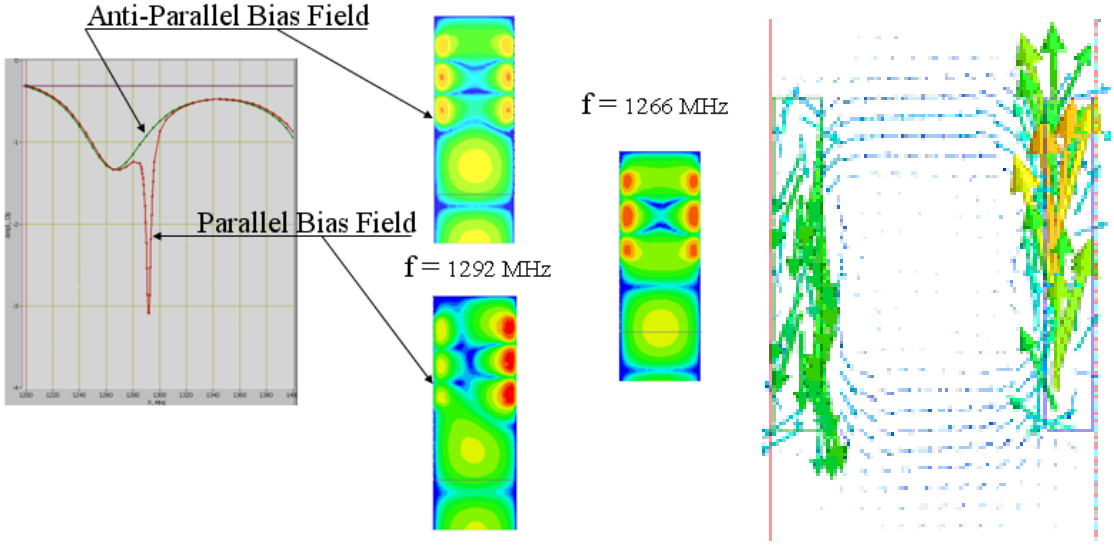

Fig. 2: Resonance associated with circular polarization

II. Matching for non-trapped modes

Let two identical ferrite blocks be positioned symmetrically in a waveguide and biased with uniform 'anti-parallel' magnetic field. Here we can expect resonance response of the system not associated with the trapped modes. The resonance conditions can be created due to poor matching of the ferrite-loaded section with the rest of the waveguide. Resonance modes in this section of the waveguide can be described in usual terms as the modes TE_{10i}, where i = 1, 2, 3, etc. Because theses modes are well coupled with the main mode TE_{10}, the width of these resonances is quite significant and associated power loss can be a limiting factor for the device performance. When the bias field changes, the magnetic permeability of the ferrite blocks also changes, resulting in the movement of the resonance frequency. When this resonance is close to the working frequency of 1300 MHz, associated power loss puts a limit to the phase shift range of the device. In principle, this type of the resonance condition can be avoided by better matching for the working mode TE_{01}.

If only this type of resonances existed in the system, one could expect the phase shift in the device close to 360°. Nevertheless, the diagrams shown in Fig. 3 [1] shows that during the first high power test, the phase shift was limited to ~90°. Although this phase shift was close to what was required, understanding limiting factors and using this understanding to improve performance of the device seemed important.

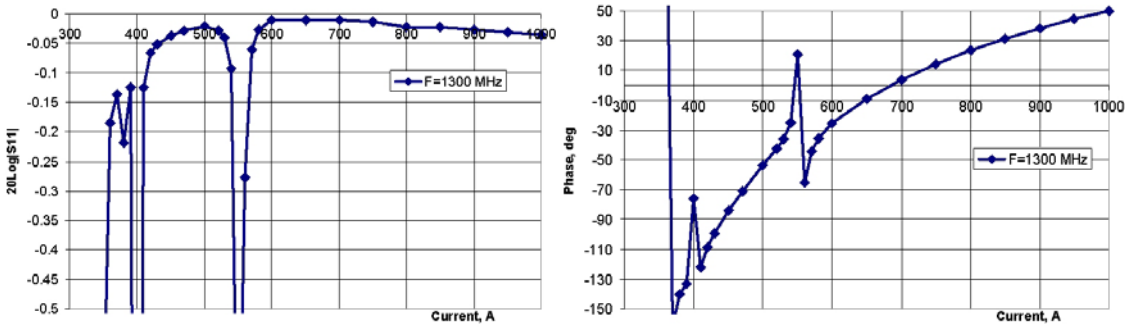

Fig. 3: Low level RF power loss and phase diagrams of the prototype phase shifter shown in Fig. 1.

III. Asymmetry in positioning and biasing the ferrite blocks

Simulation and low level RF measurements showed that in cases when some asymmetry in placing the ferrite blocks exists, or if magnetic field is slightly different in different blocks, more modes couple with the TE_{10} mode propagating in the waveguide. In this case, the phase shift range (a criterion for the edge of the range is certain level of power loss) can become narrower, which obviously was observed during the first test of the system. There were several additional trapped modes found that could have resonant frequencies of 1.3 GHz at some asymmetry of bias or positioning.

a) TE_{20} modes

With symmetrical block positioning and equal magnetic field in the blocks, TE_{20} mode is not coupled with the main mode: coupling with one of the blocks is cancelled by coupling with another one. By introducing a ±1% bias asymmetry (e.g. 800 ± 8 Oe) coupling through electric and magnetic field is made possible. As a result, TE_{202} trapped resonance condition can exist at 1240 MHz. Magnetic field of this mode is shown in Fig. 4. By changing the bias field, it is possible to move this resonance to 1300 MHz.

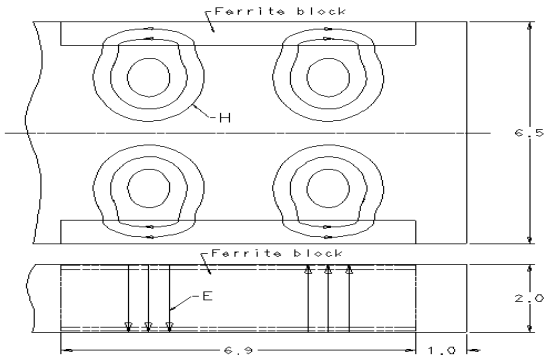

Fig. 4: Magnetic field distribution for the oscillation mode TE_{202} (trapped)

Near the working frequency, a mode similar to shown in Fig. 4, but with three variations along the length can exist. In the case of the asymmetric bias, it is also coupled to the main mode. With ± 1% of a bias asymmetry around 800 Oe and with symmetrical positioning of the blocks, there is a resonance of TE_{203} type at 1368 MHz. This mode is shown in Fig. 5 below.

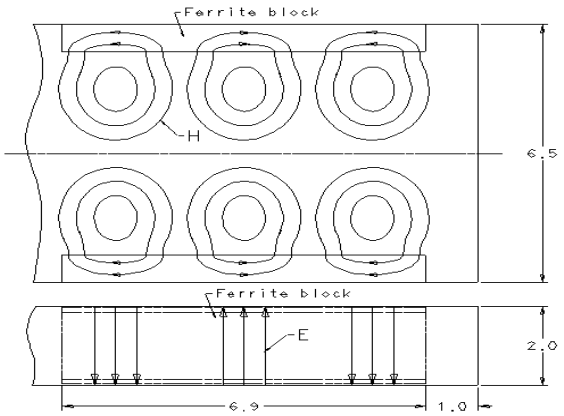

Fig. 5: Magnetic field distribution for the oscillation mode TE_{203} (trapped)

b) TE_{11} modes

Presence of ferrite blocks in the waveguide makes it possible for the modes with variations along Y axis to exist. One of examples is shown in Fig. 6 for the case of TE_{111} mode.

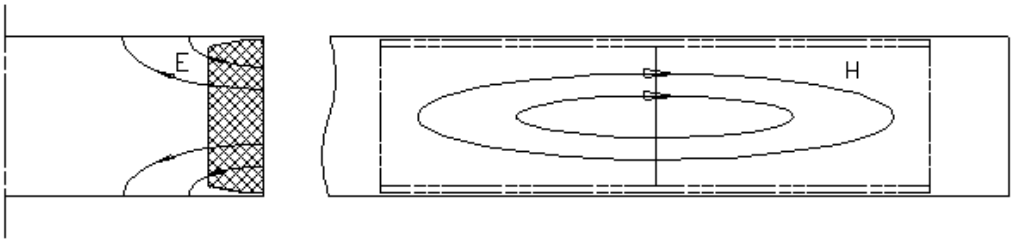

Fig. 6: Magnetic and electric field distribution for the oscillation mode TE_{111}

In this case, medium section of the waveguide (in the transverse direction) is impassible for the wave and two independent resonant circuits exist in the vicinity of the ferrite blocks that can be excited independently. It means that in reality it is not exactly TE_{111} mode, but rather two separate quarter-wave TE_{111}-like modes. When a block is positioned symmetrically, there is no coupling with the TE_{10} mode. Shifting the block up or down provides some coupling. If the bias value is changed in any block, corresponding resonant frequency also changes. For example, with vertical displacement of 1 mm for both blocks and with ± 1% of bias asymmetry

around 800 Oe, we find resonance frequency for one block at 1300 MHz and for another block – at 1307 MHz.

In Fig. 7, distribution of magnetic and electric field is shown in the case of a similar resonance mode with two variations along Z axis: TE_{112}.

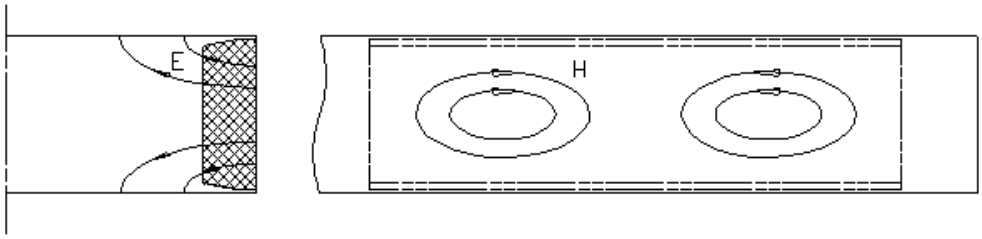

Fig. 7: Magnetic and electric field distribution for the oscillation mode TE_{112}

With 800 Oe bias for both blocks and with 1-mm block vertical shift, resonance condition occurs at 1356 MHz.

IV. Compensation for coupling

Besides asymmetry in positioning and bias field, small variations of properties of the ferrite blocks can result in additional coupling with the main mode. A way must be found to deal with this unwanted coupling.

The most obvious measure is to ensure proper block positioning during fabrication by applying strict fabrication tolerances to the assembly. This way has proved to be effective for TE_{11} resonant modes. To compensate for different material properties of the blocks or slightly different bias levels, compensation coils were introduced (see Fig. 8) that allowed independent adjustment of magnetic field in the gaps. Besides the compensation coils, thinner ferrite blocks were used (to avoid certain resonances), and the blocks were shaped as trapezoids to reduce sparking near the resonances.

To check on the magnitude of possible coupling effects and effectiveness of different compensation techniques, a series of low level RF measurements was conducted. Fig. 9 shows reflective wave amplitude diagrams (log scale) for the system shown in Fig. 8 built by using a network analyzer. Trapezoidal cross-section, 17.8 mm thick YIG blocks were used in this setup. With the current in the main winding of ~380.5 A, a bias magnetic field of ~837 Oe in the magnet gap (flux density of about ~1407 Gs in the blocks) was created. Up to ±10% adjustment of the magnetic field in each gap could be achieved by changing current in the correction winding.

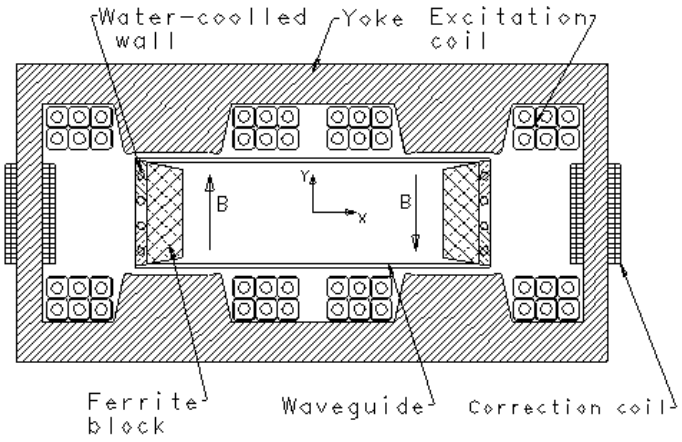

Fig. 8: Phase shifter cross-section with correction coils

Wile describing the resonance properties of the system, we will use currents as an argument. Oscillation modes shown in the graph in Fig. 9 correspond to the modes described above. By using small non-magnetic shims, each ferrite block was shifted 1 mm upward vertically. Green traces in the graph corresponds to the bias I_b = 380.5 A without correction (I_c= 0). Red lines in the four diagrams in Fig. 9 correspond to different settings of current in the correction coil: 3 A, 5.1 A, 7.0 A, and 7.7 A.

Mode TE_{202}

Because TE_{202} mode does not have variations along Y axis, it is not coupled to the main mode if bias is symmetrical even if there is some vertical displacement of the blocks. What we see on the green curve at 1240 MHz means that there is some difference in magnetic field or in the magnetic properties of the blocks. Because for this mode the two blocks belong to the same resonance circuit, only one resonance exists (1240 MHz). After compensation current I_c = 3 A was applied, this mode became less coupled that resulted in a better quality factor and increased power loss. With 5.1 A in the compensation coil, the coupling is further reduced and becomes close to optimal, with coupling coefficient $\kappa = 1$. Further increase of the compensation current leads to further reduction of coupling to the extent when at 7.7 A there is no coupling at all. This mode is not visible in the corresponding graph, so this compensation method works quite well.

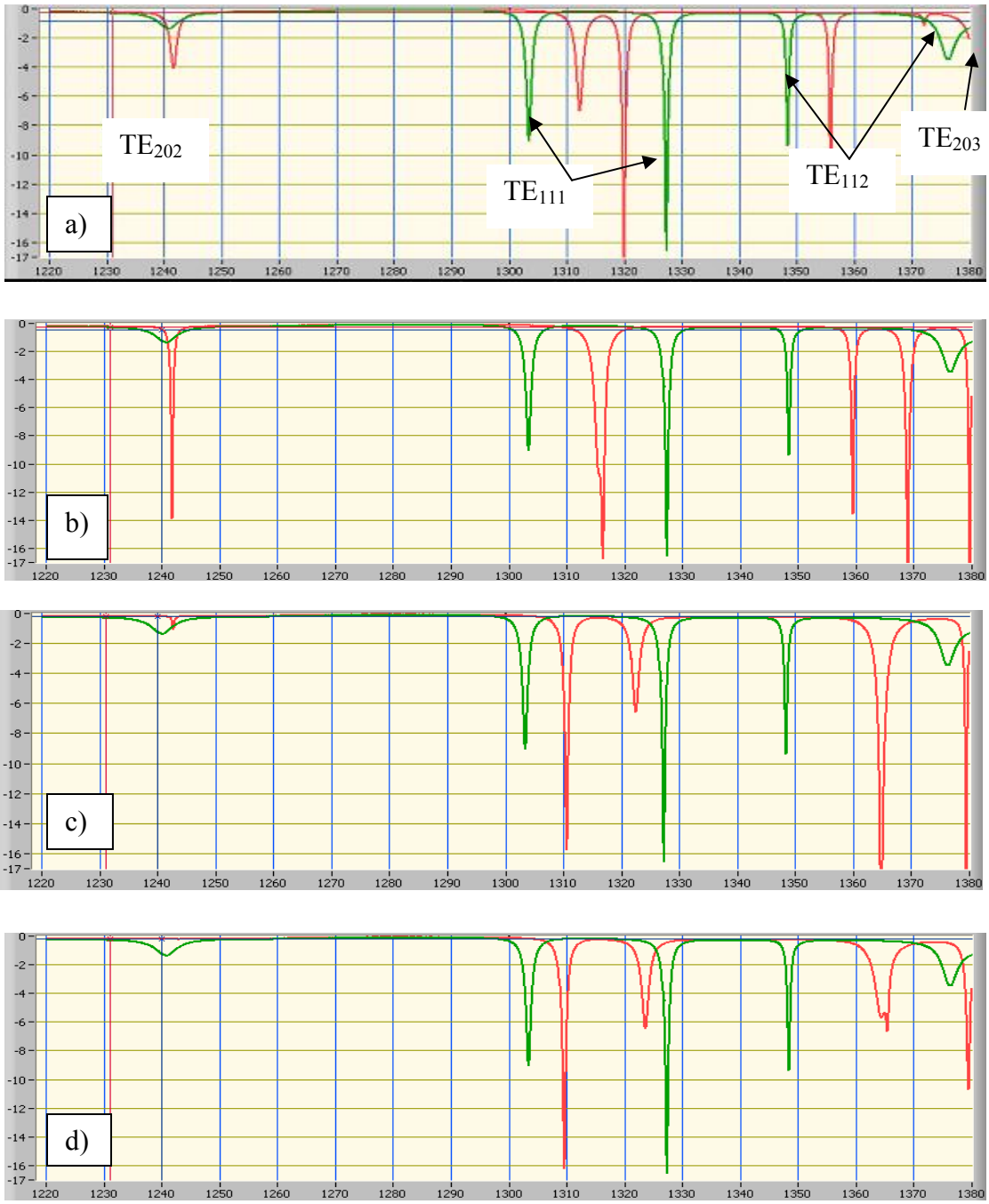

Fig. 9: I_b = 380.5 A; shift s = 1 mm; I_c = 0 A for the green reference line. a) I_c = 3 A; b) I_c = 5.1 A; c) I_c = 7.0 A; d) I_c = 7.7 A.

Mode TE_{203}

Behavior if the TE_{203} mode is similar to that of the TE_{202} mode. The resonance frequency is ~1380 MHz, so it is on the other side of the phase shift range. The same compensation method can be applied to reduce the coupling, but the compensation is reached at different current level.

Mode TE_{111}

Due to the relative vertical shift of the blocks, there is always coupling between this and the main mode. There are two split frequencies for the mode TE_{111} that correspond to two different blocks. Without correction, the frequencies are 1303 MHz and 1327 MHz. This frequency difference can result from different bias field levels in the gaps or from different material properties of the blocks. As a result of compensation, the frequencies of the two sub-modes become first closer (I_c = 3 A) and then equal to each other (I_c = 5.1 A). At higher I_c they start separating again. It is impossible to zero coupling for this mode only by regulating the bias magnetic field.

Mode TE_{112}

As in the previous case, there is always coupling between this and the main mode due to vertical block shift, and there are two split resonance frequencies corresponding to resonances in each block (in this case, without correction, they are 1348 MHz and 1376 MHz). These frequencies can be made equal (I_c = 7.0 A), but the two resonances will never cancel each other.

So, as we saw, by adjusting the magnetic field in the gaps of the magnet we could fully decouple modes TE_{20} from the main mode TE_{10}. We could not decouple the main mode from the mode TE_{11} this way though. Only by placing the blocks symmetrically can we reach full decoupling. This statement was verified by repositioning the blocks; by changing the vertical shift, coupling of the mode TE_{11} with the main mode was reduced to the extent of almost complete compensation. This is demonstrated by graphs in Fig. 10. The green traces correspond to the initial case of 1-mm upward shifted blocks. The red traces correspond to different values of the vertical shift, which is equal for both blocks in the waveguide.

Both TE_{111} and TE_{112} modes become less coupled to the main waveguide mode as the vertical shift of the blocks changes. Although split frequencies still tell that there can be different bias field seen by the blocks, it was possible to reach almost perfect decoupling by centering the blocks, which were almost identical in dimensions. Negative value of the shift at the point when the decoupling was reached can be explained by lack of knowledge of the initial position of the blocks.

The fact that it appeared possible to decouple TE_{11} modes by vertical centering the blocks in the waveguide provides an opportunity for independent decoupling of the resonance modes in the phase shifter.

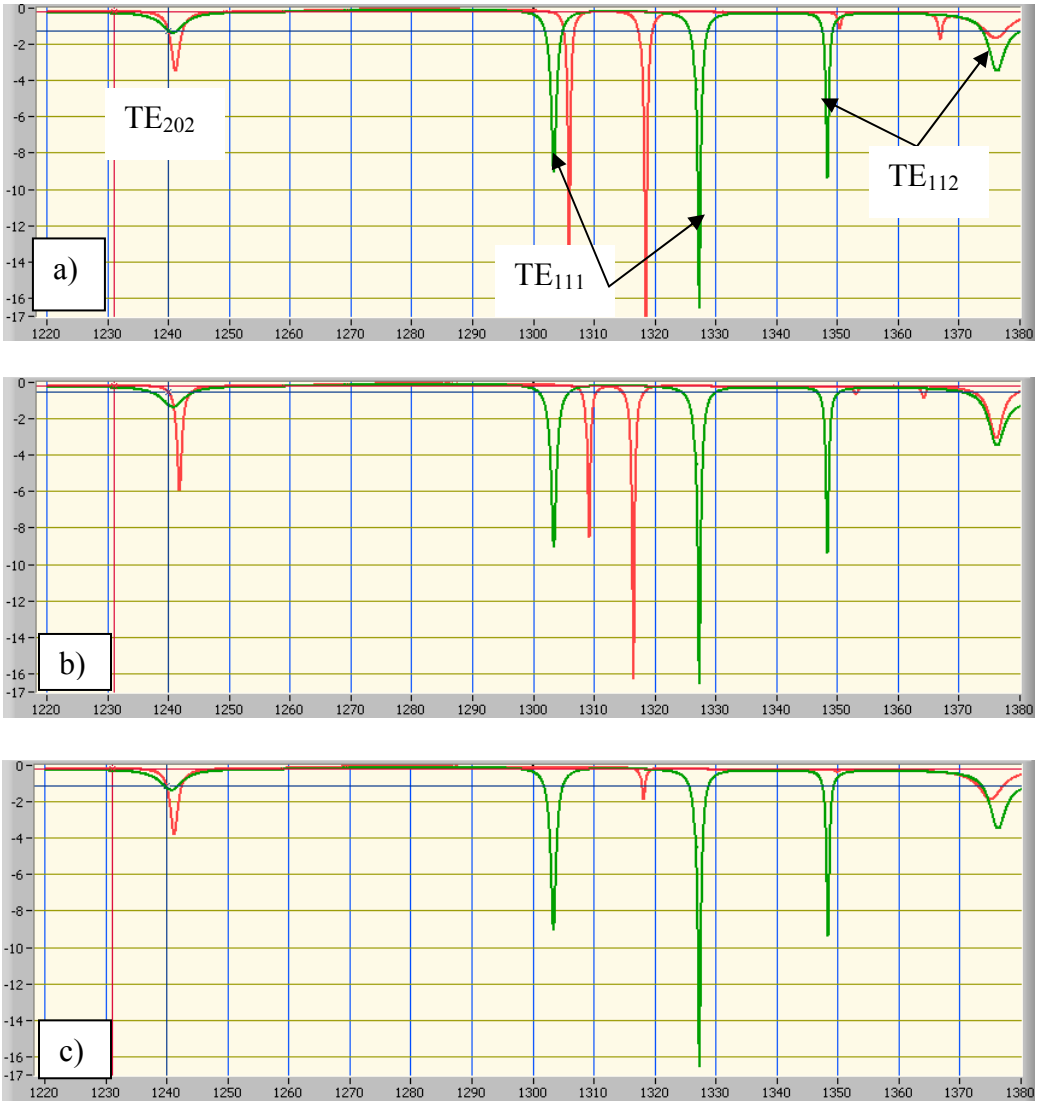

Fig. 10: I_b = 380.5 A; I_c = 0 A; shift s = 1 mm for the green reference line.
a) s = 0.5 mm; b) s = 0.3 mm; c) s = - 0.25 mm

Having TE_{11} modes decoupled, we can try to decouple TE_{20} mode by using correcting coil. Fig. 11 shows the amplitude and phase diagrams in the case when the frequency of the mode TE_{202} was set close to the working frequency 1300 MHz by changing the bias field. As it was possible to expect, vertical movement of the blocks made little effect on the main mode coupling with the TE_{20} resonance modes.

By applying the correction current I_c = 6.4 A, coupling with this mode was fully eliminated. As a result, the higher bias field region of the device (which was closed before by the TE_{202} resonance) is open now; so the phase shift range becomes larger.

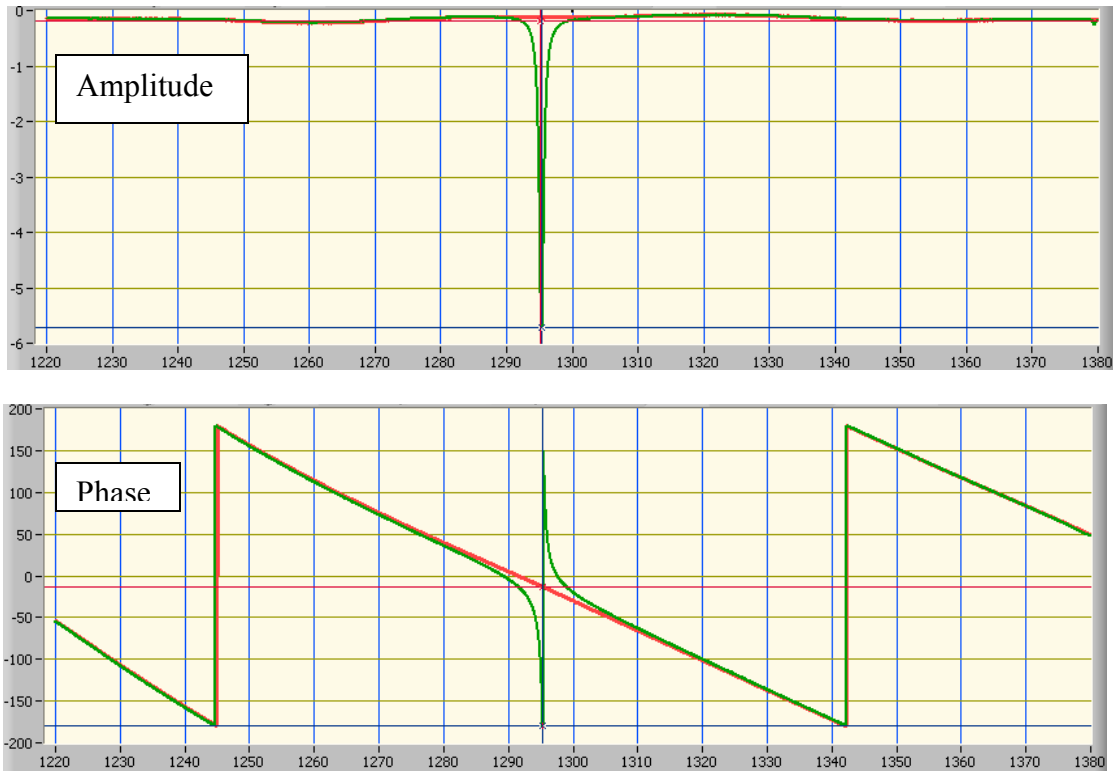

Fig. 11: Reflected wave amplitude and phase diagrams. I_b = 496A; I_c = 0 for the green reference trace; I_c = 6.4 A for the red trace

Now, after the correction is applied, there are no visible coupled modes above and below the working frequency, so both directions can be used for phase adjustment.

V. Phase Shifter Design Approach

Fig. 12 shows measured reflected wave amplitude and phase diagrams for phase shifter with 17.5 mm thick blocks. The bias current was changed in the range from 319 A to 496 A and no correction current was applied. Current limits were imposed by the onset of one of the resonances: TE_{202} on the high bias field side and TE_{111} on the low field side.

A section through these plots at 1300 MHz provides simplified amplitude and phase diagrams shown in Fig. 13. The scale of the vertical axis in the figure was adjusted to get symmetric phase limits.

If the limits of acceptable attenuation of the phase shifter is set to 0.2 dB, operating range of the device reaches 180° with the phase shift changing from -80° at 324 A to +100° at 496 A.

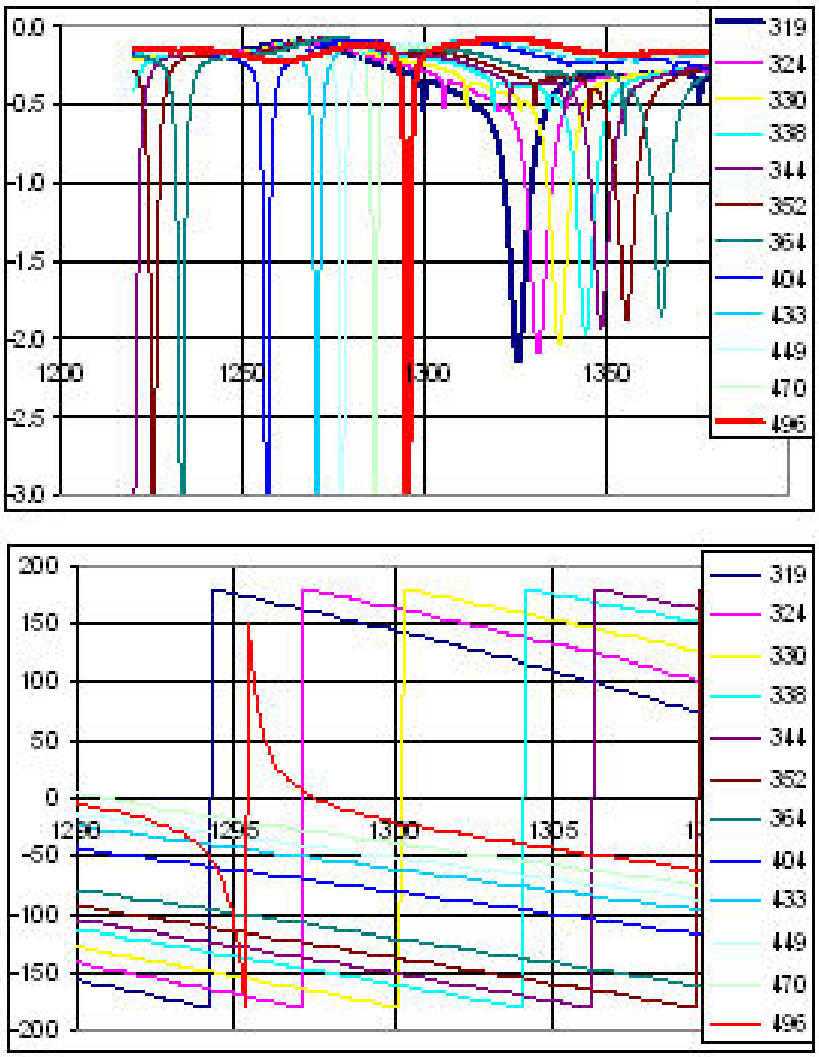

Fig. 12: Summary plots of attenuation and phase diagrams

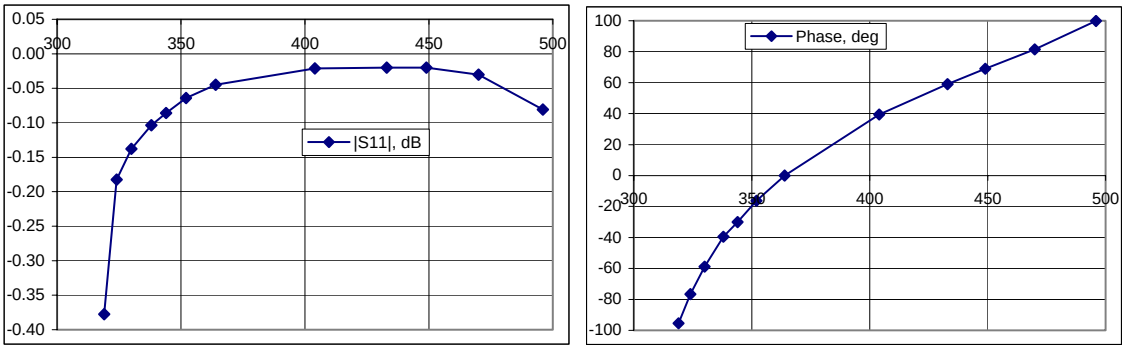

Fig. 13: Wave amplitude and phase diagrams at 1.3 GHz; t = 17.5 mm

Thickness of the ferrite blocks is important parameter to investigate. Using thinner block can improve heat transfer properties of the device, while thicker block can ensure better tuning range. Because the phase shift range obtained in this exercise is much larger than ~90° required for the linac operation and because a possible hidden advantage of using thinner blocks is making the device air-cooled instead of water-cooled, 15.5 mm thick blocks were tested to find similar properties with more modest phase shift. Amplitude and phase diagrams for this case are shown in Fig. 14.

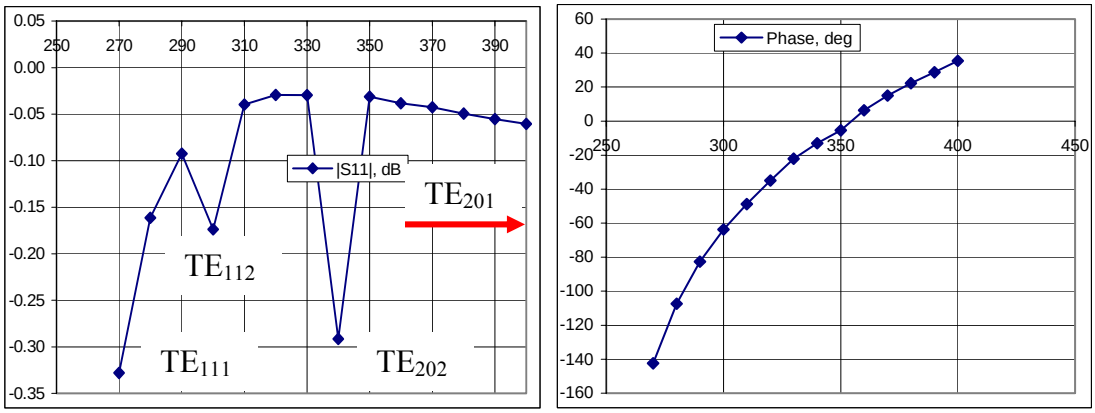

Fig. 14: Reflected wave amplitude and phase diagrams: t = 15.5 mm

In this case, no attempts were made to fully decouple modes TE_{111} and TE_{112} by vertical centering; the two modes are clearly seen in the amplitude plot. Also, neither TE_{202} nor TE_{201} modes were decoupled by adjusting the gap field using correctors. Nevertheless, even without decoupling, if the acceptable limit of power loss is set to 0.3 dB (thinner blocks provide better heat transfer) the phase range of the device is ~180° with the phase changing from -140° at 270 A to 40° at 400 A. The low current limit is set by TE_{111} trapped mode resonance. The high current limit is not seen on this graph, but can be set by TE_{201} mode. We did not make attempt to find the limiting mode on the high current side of the current interval because our goal was to move to lower bias current in order to make magnetic circuit of the device simpler.

VI. Comparing modeling and measurement results

One of major questions asked during this study was how accurately we can predict behavior of the system by modeling. Some approach to answering this question is given by the next two diagrams that compare calculated and measured properties. Because in the case of the high power test the limit to available phase shift is set by coupling with TE_{202} or TE_{111} modes, it worth to compare measured and calculated frequency shift of these modes due to bias field. Corresponding curves in Fig. 15 show good

predictability of this behavior. 17.5 mm thick blocks were used in this modeling and measurement exercise.

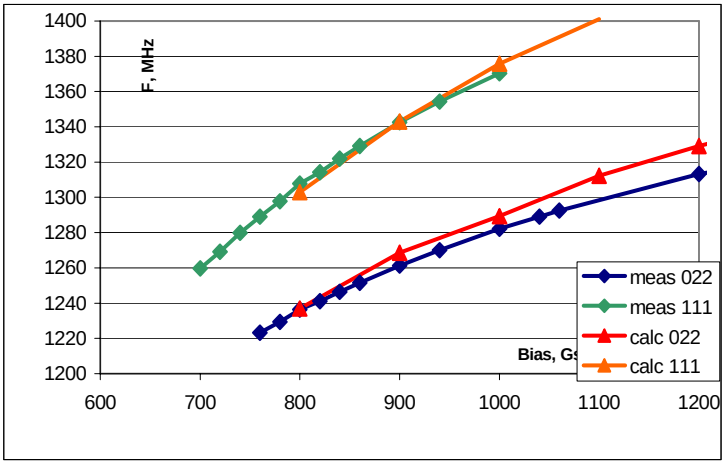

Fig. 15: TE_{202} and TE_{111} modes frequency shift

In Fig. 16 the calculated and measured reflected wave phase shift are compared at different bias levels.

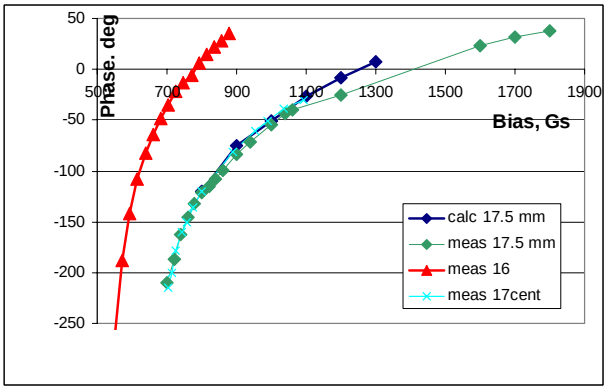

Fig. 16: Reflected wave phase shift as function of bias field

Measurement results in the cases of the centered blocks and 1 mm vertically shifted blocks also match well with the results of modeling.

VII. Summary

In our attempt to understand behavior of the mockup of a phase shifter described in [1], we have found:

1. Main limits to the device phase shift range are set by resonant conditions in the part of the waveguide with ferrite blocks for the TE_{20} and TE_{11} modes and coupling of these modes with the main waveguide mode TE_{10}.

2. The coupling can be fully eliminated by adjusting magnetic field in the ferrite blocks for the TE_{20} mode and by centering the blocks for the TE_{11} mode.
3. If proper decoupling is performed, making blocks thinner does not affect much the phase shift capability of the device. Using thinner blocks can allow shifting the bias field to lower level. At certain block thickness, onset of the gyro-magnetic resonance will become a limiting factor.
4. Modeling provides adequate information about performance of the device.
5. To continue with the development the next measures can be considered:
   - Reduction of block thickness. This leads to lower bias field and simplifies heat flux management.
   - Shortening the device. This will lower inductance and power consumption.
   - Reduction of the waveguide height. This will simplify magnetic system and reduce power consumption. Excitation of TE_{11} modes can be eliminated in this case.
   - Local reduction of the waveguide width. This will increase frequency of the TE_{20} mode and help to make compact design.
6. Modeling is required before a prototype system is designed.

References:

1. B. Foster, et al, High Power Phase Shifter, Proceedings of 2005 Particle Accelerator Conference, Knoxville, TN, 2005, pp. 3123 – 3125.
2. B. Foster, et al, High Power Phase Shifter for Application in the RF Distribution System of Superconducting Proton Linac, HPSL-2005, Naperville, May 22-24, 2005.
3. J.L. Wilson, et al, “Development of High Power RF Vector Modulator Employing TEM Ferrite Phase Shifter”, LINAC 2006, Knoxville, TN, 2006, Proceedings, pp. 451 – 453.
4. Y.W. Kang, et al, “Development and Testing of High Power RF Vector Modulators”, Proceedings of 2007 Particle Accelerator Conference, Albuquerque, NM, 2007, pp. 2508 – 2510.
5. D. Valuch, “A Fast Phase and Amplitude Modulator for the SPL”, HPSL-2005, Naperville, May 22-24, 2005.